Design and Analysis of a Transverse Flux Machine with Soft Magnetic Composite Core

Youguang GUO[1], Jian guo ZHU[1], Peter A. WATTERSON[1], and Wei WU[2]
[1]Faculty of Engineering, University of Technology, Sydney, P.O. Box 123, Broadway, NSW 2007, Australia
Phone: 61-2-95147903 Fax: 61-2-95142435 E-mail: youguang@eng.uts.edu.au Website: http://www.eng.uts.edu.au/~joe
[2]CSIRO Telecommunications and Industrial Physics, P.O. Box 218, Lindfield, NSW 2070, Australia

***Abstract*-This paper presents the design and performance analysis of a three phase, three stack permanent magnet transverse flux motor with soft magnetic composite core. To predict and optimize the major parameters, three-dimensional finite element analysis is performed. The performance is calculated when the motor operates with a brushless DC drive.**

I. INTRODUCTION

Soft magnetic composite (SMC) materials have unique properties that may offer a revolution in the design and manufacture of electrical machines [1]. The unique properties include three-dimensional (3D) isotropic ferromagnetic behaviour, very low eddy current loss, relatively low total iron loss at medium and high frequencies, possibilities for improved thermal characteristics, flexible machine design and assembly, and a prospect for greatly reduced production costs. To investigate the potential of SMC materials, a lot of work has been conducted and some improvement has been achieved both in the material and its application in electrical machines [2,3].

This paper presents an investigation on a 3-phase 3-stack permanent magnet (PM) transverse flux motor with SMC core. SOMALOY™ 500, a new soft magnetic composite produced by Höganäs AB, Sweden, is used as the core material. SMC is made of coated pure iron powder with high compressibility. The coated powder is pressed in a die to form solid net shape and heat treated to anneal and cure the bond.

Compared with electrical steels widely used in rotating machines and transformers, the major advantages of SMC materials is the prospect of large volume manufacturing of low cost electromagnetic devices. Because the iron cores and parts can be pressed in a die into the desired shape and dimension, the further machining is minimized and hence the production cost is greatly reduced. Magnetically, the coated powdered nature of the material means low eddy current loss and isotropic magnetic properties, and therefore, it is especially suitable for construction of 3D flux devices such as claw pole and transverse flux machines. In these machines, it is very difficult to use laminated steels. Because the permeability of SMC materials is lower than that of electrical steels, it is expected that SMC would be most appropriate for PM machines for which the magnetic reluctance of the magnet dominates the magnetic circuit, making such motors insensitive to the permeability of the core.

This paper obtains the magnetic field through 3D finite element method (FEM) and then calculates the major motor parameters. The **B-H** characteristics and rotational core losses of SOMALOY™ 500 with rotating magnetic fluxes at different frequencies were measured using a single sheet rotational core loss tester and applied in the magnetic field analysis and performance calculation [4].

II. STRUCTURE AND DIMENSIONS

Since Weh proposed the first two versions of transverse flux machines (TFM) featuring high power density and high efficiency [5], PM machines with transverse flux structure are attracting increasing attention. Motors of this type could produce very high torque or force at low speeds and could find wide application in direct drives.

The magnetically relevant parts of the TFM type chosen here are shown in Fig. 1, and the dimensions and major parameters are listed in Table I.

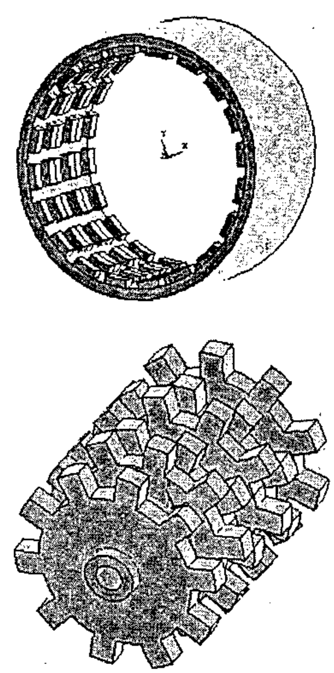

Fig. 1. Magnetically relevant parts of the TFM prototype

TABLE I
DIMENSIONS AND MAJOR PARAMETERS

Dimensions and parameters	Quantities
Rated frequency (Hz)	300
Number of phases	3
Rated power (W)	690
Rated line-neutral voltage (V)	80
Rated phase current (A)	5
Rated speed (rev/min)	1800
Rated torque (Nm)	3.67
Rated efficiency (%)	88.7
Rated temperature rise (°C)	75
Number of poles	20
Stator and rotor core material	SOMALOY™ 500
Stator outer radius (mm)	40
Effective stator axial length (mm)	93
Rotor outer radius (mm)	48
Rotor inner radius (mm)	41
Permanent magnets	NdFeB, Grade N30M
Number of magnets	120
Magnet dimensions	OD88 x ID82 x 9 mm arc 12°
Magnetization directions	Radially outward or inward
Main airgap length (mm)	1
Stator shaft	Mild steel
Shaft outer radius (mm)	9.5
Number of coils	3
Coil window dimension (mm²)	16 x 20.5
Number of turns	125
Number of strands	2
Diameter of copper wire (mm)	0.90

The motor phases are stacked axially, and alternative phase numbers could be chosen. The motor has an outer rotor comprising a tube of SMC with two rings of magnets per phase mounted on the inner surface. SMC is used for the rotor yoke because of oscillating flux density. Each stator phase has a single coil around an SMC core, which would be molded in two halves. If the phase stator cores were touching, flux could pass between the phases, significantly increasing inductance. To avoid this, thin copper or aluminum sheets can be included between the phases to make them essentially independent. The sheet has very high electrical conductivity and the induced eddy currents will prevent varying flux from penetrating through the sheet.

The motor size and core geometry were determined by the dimensions of the available SOMALOY™ 500 preforms. They are the same as those of a claw pole SMC prototype, enabling comparison [6]. A pole number of 20 was chosen giving an operating frequency of 300 Hz at 1800 rpm. It is not an unrealistically high frequency to work at for SMC materials.

III. 3D FEM MAGNETIC FIELD ANALYSIS

The magnetic flux path in the TFM is predominantly in planes containing the axis but becomes 3D as it spreads azimuthally to reduce flux densities. For non-linear material properties and accurate flux fringing calculation, a 3D finite element analysis is required. Here, the commercial software package ANSYS was used. In the design of this prototype, the dimensions and parameters of the motor were first approximately determined by magnetic circuit analysis and then refined by the finite element analysis.

Taking advantage of the periodical symmetry, only one pole-pair region of the machine, as shown in Fig. 2, needs to be studied.

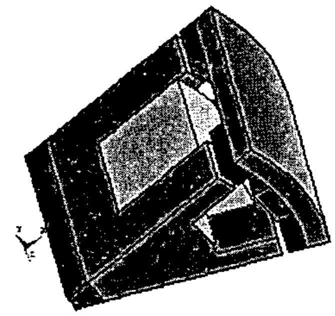

Fig. 2. Region for field solution

At the two radial boundary planes, the magnetic scalar potential obeys the periodical boundary conditions:

$$\varphi_m(r,\Delta\theta,z)=\varphi_m(r,-\Delta\theta,z) \tag{1}$$

where $\Delta\theta = 18°$ is the angle of one pole pitch.

A. *No-load Magnetic Field Distribution*

The no-load magnetic field distribution is calculated to find out the magnetic flux linking the stator winding and hence the induced *emf* due to the rotation of the permanent magnets on the rotor. The motor structure should be adjusted such that the flux linkage of the stator winding is the maximum. As plotted in Fig.3, this flux waveform is almost perfectly sinusoidal versus the rotor position.

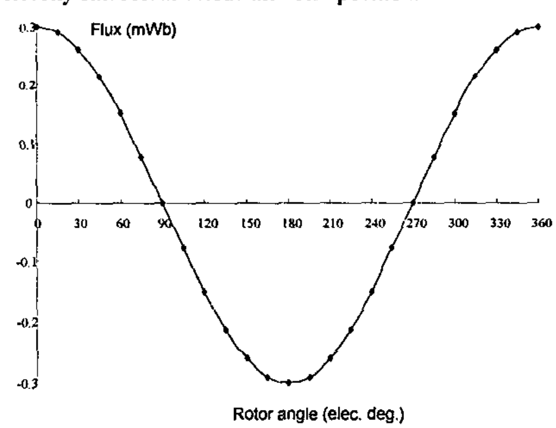

Fig. 3. No-load flux per turn of a phase winding

B. *Cogging torque*

Cogging torque is caused by the tendency of the rotor magnets to line up with the stator poles where the magnetic circuit has the highest permeance when the motor is under no-load. Fig. 4 shows the cogging torque variation versus the rotor position for one phase of the machine, calculated by the Coulomb virtual work method.

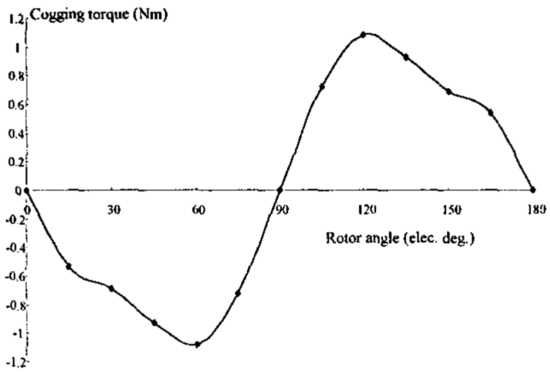

Fig. 4. Cogging torque versus rotor angle for one stack

The cogging torque has period 180 electrical degrees and anti-symmetry about zero, hence only even sine harmonics, which were computed by the Discrete Fourier Transformation (DFT) method to be

$$T_A \approx -1.0303\sin 2\theta + 0.1677\sin 4\theta - 0.1130\sin 6\theta - 0.0574\sin 8\theta - 0.0107\sin 10\theta + 0.0001\sin 12\theta \quad (2)$$

where θ is the rotor angle in electrical degrees. The stator teeth on the three phases are shifted by 120 electrical degrees, and all even harmonics other than order 6 or its multiples sum to zero over the three phases. The magnitudes of the 6^{th} and 12^{th} harmonics of cogging torque are 0.3390 Nm and 0.0003 Nm, respectively. These values are quite small compared with the rated torque of 3.67 Nm and hence do not have a significantly detrimental effect on the motor operation.

C. Inductance and Armature Reaction

The self- inductance of each phase can be calculated by

$$L_1 = \frac{N_1 \phi_1}{I_1} \quad (3)$$

where ϕ_1 is the magnitude of the flux linking the stator winding due to a stator current I_1 in N_1 turns. It can be obtained from the results of a field analysis with stator current I_1 and the permanent magnets "switched off", i.e. remanence set to zero. In this three-phase motor, the mutual inductance between phase windings can be considered as zero since the magnetic circuit for each phase is basically independent. From Table II, it can be seen that the inductance is very uniform with rotor angle. The inductance scales as N_1^2 and so is 6.08 mH for 125 turns. It is also shown in Table II that the armature reaction for rated current is quite small and it will not demagnetize the magnets.

TABLE II
PER-TURN INDUCTANCE AND ARMATURE REACTION IN MAGNETS

Rotor position (electrical degrees)	Self inductance (μH)	Maximum B in magnets (Tesla)
0	0.3890	0.099
30	0.3888	0.099
60	0.3886	0.102
90	0.3888	0.099

D. Core Loss Calculation

The local flux density patterns within a 3D-flux machine are quite complex [7]. The flux density locus at one position can be alternating (1D) with or without harmonics, 2D or even 3D rotating with purely circular or elliptical patterns. Experiments on samples revealed significant difference between the core losses caused by alternating and by rotating magnetic fields [4].

An improved method is applied for predicting iron losses of 3D-flux SMC machines in [8,9]. Different formulations are used for iron loss prediction with purely alternating, purely circular rotating, and elliptically rotating flux density vectors, respectively. A series of 3D finite element analyses are conducted to determine the flux density locus in each element when the rotor rotates. The calculated no load iron loss, varied approximately linearly with frequency and was 29 W at 300 Hz. Under rated load it will increase by about 20%.

E. Optimization of magnet length

Taking advantage of the isotropic magnetic property of SMC material, the magnet length can be chosen longer than the tooth width to obtain higher stator flux and then higher specific torque. However, too much magnet overhang may lead to over saturation and is cost-ineffective. Fig. 5 illustrates the ratio of total material cost and electromagnetic torque versus the magnet axial length.

F. Flux Penetration in Stator Shaft

In the field analysis, the flux is considered not to pass through the stator shaft since the mild steel shaft has much higher conductivity and permeability than the SMC yoke, as shown in Table III.

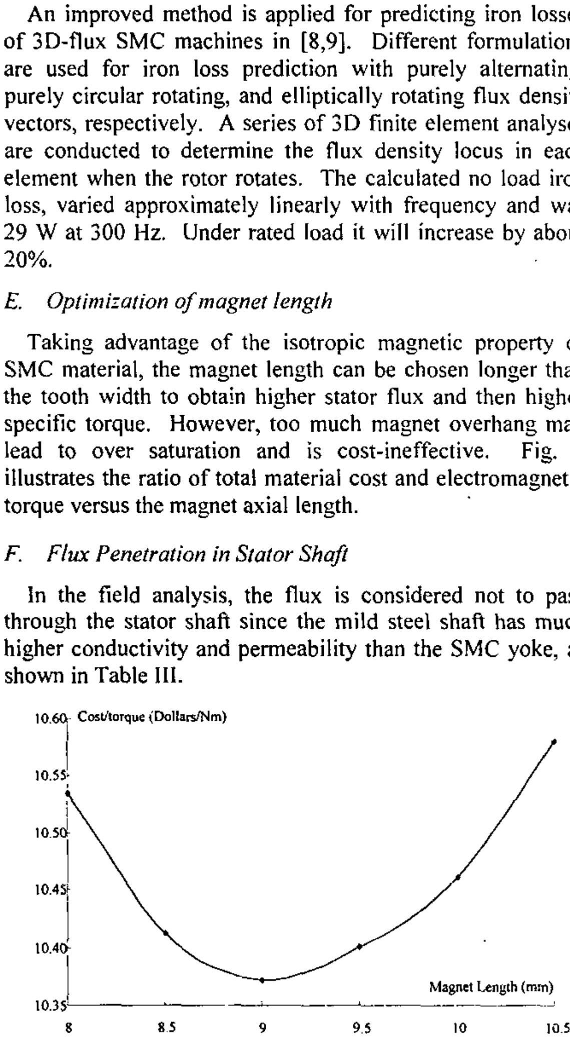

Fig. 5. Cost/torque versus magnet length

TABLE III
COMPARISON OF SMC AND MILD STEEL

Parameters	SMC	Mild steel
Relative permeability	130	5000 (range 1500 – 10000)
Conductivity (S/m)	500 - 10000	1.12×10^7
Penetration or skin depth at 300 Hz (mm)	25.5 – 114	0.123

The penetration or skin depth can be calculated by

$$\delta = \sqrt{\frac{2}{\omega\mu\sigma}} \tag{4}$$

where μ is the magnetic permeability of the material, σ the electric conductivity, and ω the angular frequency of the flux. The flux penetrating the shaft and the eddy current loss are given by, assuming linear permeability, [10]

$$\phi = B_p(2\pi r_{shaft})\frac{\delta}{\sqrt{2}} \tag{5}$$

$$w_e = \frac{B_p^{\,2}}{2\mu^2\sigma\delta}(2\pi r_{shaft} l_{shaft}) \tag{6}$$

where B_P is the peak flux density just inside the shaft surface, r_{shaft} is the shaft radius, and l_{shaft} is the effective shaft length. The maximum flux density in the stator yoke is about 1.0 T, kept low to reduce core loss. By continuity of tangential magnetic field strength, B_P will be saturated, around 2 T. Though Eq. (5) and Eq. (6) are for non-saturated material, if applied they give that the penetrating flux and eddy current loss in the mild steel shaft at 300 Hz are only 0.005 mWb and 0.051 W, respectively. Compared to the flux and core loss in the SMC yoke, these values are negligible.

G. *Eddy Current in SMC*

Since it is very difficult to model the complex cyclic magnetization of SMC in the FEM magnetic field analysis, a single valued B-H curve is used instead and iron loss is then estimated as a post-processor exercise. There is a risk for design using SMC in this approach associated with eddy current [2]. The insulation between grains in SMC is not perfect and significant bulk eddy current, which flows between grains, may well be present. The ratio of the material dimensions to skin depth is a critical parameter. If the smallest dimension of the component normal to the magnetic field plane is near the skin depth the field will be significantly disturbed by the eddy currents and will be restricted to near the surface of the component. The result is that the effective permeability falls, a phase shift is introduced, high loss is induced, and the skin effect must be part of the analysis, which is far more complex.

The narrowest dimensions for the SMC stator teeth, the stator yoke, and the rotor yoke are 8 mm, 10 mm and 4 mm, respectively. They are much lower than the skin depth at the rated frequency, as in Table III. Thus, the magnetic field analysis can be conducted ignoring eddy currents.

IV. PERFORMANCE CALCULATION

The motor uses a standard six-transistor bridge drive circuit. With open-loop control, the motor can operate in normal synchronous mode. With the closed-loop control of position feedback it can also operate in brushless DC mode where the current I_1 and the induced *EMF*, E_1 in the stator winding are aligned for maximum electromagnetic power P_{em} at a given speed

$$P_{em} = 3E_1 I_1 \tag{7}$$

The induced stator *EMF* can be determined by

$$E_1 = \frac{\omega_1 N_1 \phi_m}{\sqrt{2}} \tag{8}$$

where $\omega_1 = 2\pi f_1$ is the angular rotor speed in electrical radians per second, f_1 the frequency of the induced stator *EMF* in Hertz, N_1 the number of turns of the stator winding, and ϕ_m the magnitude of the magnetic flux linking the stator winding due to the permanent magnets.

At 1800 rpm (300Hz), E_1= 50 V, and for the expected rated current 5 A, limited by the temperature rise of the stator winding, P_{em}=750 W. The rated line-neutral rms voltage is:

$$V_1 = \sqrt{(E_1 + I_1 R_1)^2 + X_1^{\,2}} \tag{9}$$

where R_1 is the resistance of one phase winding and X_1 is the reactance. The corresponding DC input voltage of the inverter can be estimated by [11]

$$V_{dc} = 2.34 V_1 \tag{10}$$

to be 189 V, though this formulae was derived for no load.

The output power, output torque, input power, and efficiency are calculated by

$$P_{out} = P_{em} - P_{core} - P_{mec} \tag{11}$$

$$T_{out} = P_{out} / \omega_r \tag{12}$$

$$P_{in} = P_{em} + P_{cu} \tag{13}$$

$$P_{cu} = 3 I_1^{\,2} R_1 \tag{14}$$

$$\eta = P_{out} / P_{in} \tag{15}$$

where P_{core} is the core loss, P_{mec} the mechanical loss, P_{cu} the copper loss, and ω_r is the angular speed. The temperature rise is calculated by using an equivalent thermal circuit where these losses are the thermal sources [6].

At a given voltage input, the steady state characteristic with optimum feedback can be predicted by

$$\omega_r = \frac{V_1}{K_e} - \frac{R_1}{K_e K_T} T_{em} \tag{16}$$

where K_e is the back *EMF* constant, K_T the torque constant, and T_{em} is the electromagnetic torque.

V. CONCLUSION AND DISCUSSION

To investigate the potential of SMC materials in manufacturing of small motors of complex structures, a small 3-phase PM transverse flux motor with SMC core has been designed. The prototype is being constructed and the prototype performance is expected to be comparable to that of similar motors with electrical steel cores at potentially reduced manufacturing cost. The method for the motor design and performance analysis has been validated by the experiment on a 3-phase 3-stack claw pole PM SMC motor [6].

ACKNOWLEDGMENT

The authors would like to thank Höganäs AB, Sweden, for supplying preforms of SOMALOY™ 500.

REFERENCES

[1] A.G. Jack, "Experience with the use of soft magnetic composites in electrical machines", *Proceeding of International Conference on Electrical Machines*, Istanbul, Turkey, 1998, pp. 1441-1448.

[2] P. Jansson and A. Jack, "Magnetic assessment of SMC materials", *Twenty First Annual Conference on Properties and Applications of Magnetic Materials*, Chicago, May 2002, pp. 1-9.

[3] T.J. Hammons, H.B. Ertan, J.A. Tegopoulos, W. Drury, M. Ehsani, T. Nakata, and A.G. Jack, "1998 ICEM review", *IEEE Power Engineering Review*, February 1999, pp. 12-17.

[4] J.G. Zhu, J.J. Zhong, V.S. Ramsden, and Y.G. Guo, "Power losses of composite soft magnetic materials under two dimensional excitations", *Journal of Applied Physics*, USA, Vol.85, No.8, April 1999, pp.4403-4405

[5] H. Weh, H. Hoffmann, and J. Landrath, "New permanent magnet excited synchronous machine with high efficiency at low speed", in *Proceeding of International Conference on Electrical Machines*, 1988, pp. 35-40

[6] Y.G. Guo, J.G. Zhu, P.A. Watterson, and W. Wu, "Design and analysis of a three-phase three-stack claw pole permanent magnet motor with soft magnetic composite core", *Proceeding of Australasian Universities Power Engineering Conference*, 28 September – 1 October 2003, Christchurch, New Zealand.

[7] Y.G. Guo and J.G. Zhu, "Magnetic field calculation of claw pole permanent magnet machines using magnetic network method", *Journal of Electrical & Electronic Engineering Australia*, Vol.22, No.1, 2002, pp. 69-76

[8] Y.G. Guo, J.G. Zhu, J.J. Zhong, and W. Wu, "Core losses in claw pole permanent magnet machines with soft magnetic composite cores", *IEEE Trans. on Magnetics*, Vol.39, No.5, Sept. 2003, pp. 3199-3201

[9] Y.G. Guo, J.G. Zhu, J.J. Zhong, P.A. Watterson, and W. Wu, "An improved method for predicting iron losses in SMC electrical machines", *Proceeding of International Symposium on Applied Electromagnetics and Mechanics*, Versailles, France, 12-14 May 2003.

[10] G.W. Carter, *The Electromagnetic Field in Its Engineering Aspects*, 2nd Edition, Longmans, London, 1967, pp. 243-247

[11] P.A. Watterson, "Analysis of six-step 120° conduction permanent magnet drives", *Australasian Universities Power Engineering Conference*, 28 Sept. – 1 Oct. 1997, Sydney, Australia, pp.13-18